JOC*Note*

Schiff Base Addition to Cyclic Dicarboxylic Anhydrides: An Unusual Concerted Reaction. An MO and DFT Theoretical Study

Jose Kaneti,* Snezhana M. Bakalova, and Ivan G. Pojarlieff

Institute of Organic Chemistry with Centre of Phytochemistry, Bulgarian Academy of Sciences, Acad. G. Bonchev str., Block 9, 1113 Sofia, Bulgaria

kaneti@orgchm.bas.bg

Received February 23, 2003

Abstract: The existing controversy as to whether dicarboxylic anhydride iminolysis by Schiff bases is a concerted [4 + 2] addition or a stepwise reaction following either a Perkin-like route or occurs as iminolysis via zwitterionic intermediates is solved computationally by DFT and MO theory. Both types of theory favor a concerted mechanism starting as bimolecular addition of imine to the carbonyl carbon of anhydride monoenol, accompanied by simultaneous elimination of carboxylate. The reaction proceeds further without forming any intermediate and completes as intramolecular charge transfer from enol HOMO to imine LUMO with ring closure.

Cyclic dicarboxylic anhydrides, e.g., succinic, glutaric, or homophthalic anhydride **1**, are known to react with Schiff bases **2**, giving nitrogen heterocycles.[1−3] This addition reaction has been demonstrated to provide versatile synthetic pathways to a number of pharmacologically important compounds.[4] Accumulated experimental data on electronic and steric factors governing the reaction kinetics and its stereochemical outcome seem sufficient to its complete understanding. However, there is still controversy as to whether the reaction of aldimine with homophthalic anhydride **1** is a concerted imino Diels−Alder [4 + 2] addition[5] or is a stepwise process along either a Perkin-like mechanism[6] or an anhydride iminolysis[7] (Scheme 1).

An analysis of experimental data on steric and electronic effects on reaction stereochemistry by Cushman and Madai[7] places the first two mechanistic alternatives (Scheme 1) to the background and sugguests the zwitterionic intermediates **3** and **4**, similar to the earlier reaction of succinic anhydride.[1] Intermediates **3** and **4** arise from *Z*- and *E*-Schiff bases, respectively, and come

SCHEME 1. Three Viable Mechanisms of Schiff Base Addition to Homophthalic Anhydride 1

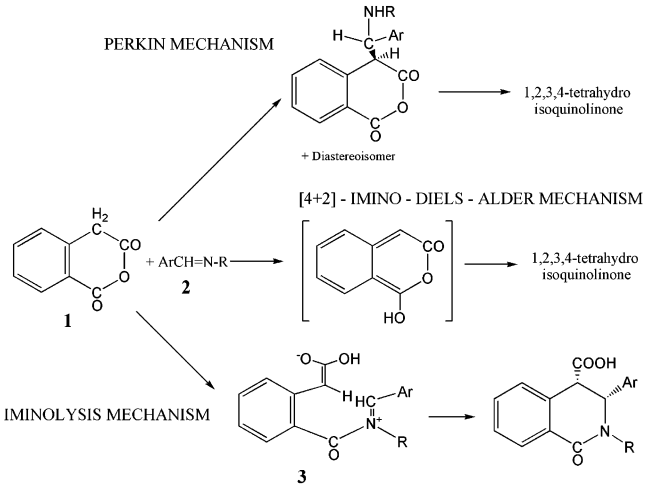

to explain the observed stereochemical outcome of *trans*- and *cis*-3,4-substituted 1,2,3,4-tetrahydroisoquinolones, respectively, from the reaction of anhydride **1**[7] and *trans*- and *cis*-4,5-substituted tetrahydropyrolidine-2-ones, respectively, from succinic anhydride **5**.[1] In both cases, the major products have the *trans*-configuration, supposedly reflecting the dominating *E*-configuration of aldimines in solution. Observed reaction product mixtures are at least partly due to the *E*−*Z* equilibrium interconversions of Schiff bases, depending on their C and N substituents as shown by NMR.[8]

The outlined addition reaction of azaethenes to anhydrides and the related mechanistic controversy attracted our interest in a theoretical study of the simplest models, succinic anhydride **5** and methylene imine **6**. The choice of succinic anhydride **5** eliminates the [4 + 2]-cycloaddition mechanism, as the corresponding diene would be its bis-enol, 2,5-dihydroxyfuran, so that the Perkin-like mechanism remains the only feasible mechanistic alternative (Scheme 1; Table S1, Supporting Information). We decided to use theoretical means[9] to pursue in more detail these two mechanistic suggestions of Cushman and Madai[7] and specifically attempt to locate the intermediates with the postulated topology of **3** and **4** on the reaction path of a stepwise process,[7] even though LFER[10] and solvent dependencies of stereochemical outcome[7] hint at a concerted mechanism.[10]

(1) Castagnoli, N., Jr. *J. Org. Chem.* **1969**, *34*, 3187.
(2) Cushman, M.; Castagnoli, N., Jr. *J. Org. Chem.* **1971**, *36*, 3404. Cushman, M.; Castagnoli, N., Jr. *J. Org. Chem.* **1972**, *37*, 1268.
(3) Haimova, M. A.; Mollov, N. M.; Ivanova, S. C.; Dimitrova, A. I.; Ognyanov, V. I. *Tetrahedron* **1977**, *33*, 331. Stanoeva, E. R.; Haimova, M. A. *Chem. Heterocycl. Compd. (Engl. Transl.)* **1984**, *20*, 1305.
(4) Kita, Y.; Iio, K.; Okajima, A.; Takeda, Y.; Kawaguchi, K.; Whelan, B. A.; Akai, S. *Synlett* **1998**, 292. Kita, Y.; Iio, K.; Kawaguchi, K.; Fukuda, N.; Takeda, Y.; Ueno, H.; Okunaka, R.; Higuchi, K.; Tsujino, T.; Fukuoka, H.; Akai, S. *Chem. Eur. J.* **2000**, *6*, 3897.
(5) Tamura, Y.; Wada, A.; Sasho, M.; Kita, Y. *Tetrahedron Lett.* **1981**, *22*, 4283. Weinreb, S. M. In *Comprehensive Organic Synthesis*; Trost, B. M., Fleming, I., Eds.; Pergamon Press: New York, 1991; pp 402−416.
(6) Shamma, M.; Tomlinson, H. H. *J. Org. Chem.* **1978**, *43*, 2852.
(7) Cushman, M.; Madai, E. J. *J. Org. Chem.* **1987**, *52*, 907.
(8) Bjorgo, J.; Boyd, D. R.; Watson, C. G.; Jennings, W. B.; Jerina, D. M. *J. Chem. Soc., Perkin Trans. 2* **1974**, 1081.
(9) Frisch, M. J.; Trucks, G. W.; Schlegel, H. B.; Scuseria, G. E.; Robb, M. A.; Cheeseman, J. R.; Zakrzewski, V. G.; Montgomery, J. A., Jr.; Stratmann, R. E.; Burant, J. C.; Dapprich, S.; Millam, J. M.; Daniels, A. D.; Kudin, K. N.; Strain, M. C.; Farkas, O.; Tomasi, J.; Barone, V.; Cossi, M.; Cammi, R.; Mennucci, B.; Pomelli, C.; Adamo, C.; Clifford, S.; Ochterski, J.; Petersson, G. A.; Ayala, P. Y.; Cui, Q.; Morokuma, K.; Malick, D. K.; Rabuck, A. D.; Raghavachari, K.; Foresman, J. B.; Cioslowski, J.; Ortiz, J. V.; Baboul, A. G.; Stefanov, B. B.; Liu, G.; Liashenko, A.; Piskorz, P.; Komaromi, I.; Gomperts, R.; Martin, R. L.; Fox, D. J.; Keith, T.; Al-Laham, M. A.; Peng, C. Y.; Nanayakkara, A.; Gonzalez, C.; Challacombe, M.; Gill, P. M. W.; Johnson, B.; Chen, W.; Wong, M. W.; Andres, J. L.; Gonzalez, C.; Head-Gordon, M.; Replogle, E. S.; Pople, J. A. *Gaussian 98*, rev. A.7; Gaussian Inc.: Pittsburgh, PA, 1998.

10.1021/jo034240j CCC: $25.00
Published on Web 07/29/2003

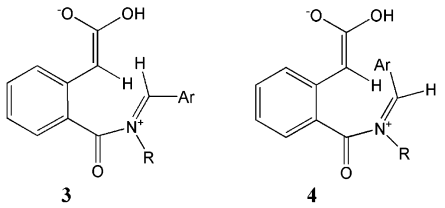

3 **4**

We consider initially two modes of imine attack on anhydride: (a) attack on a carbonyl of the entirely keto anhydride and (b) attack on the nonenolized carbonyl of anhydride monoenol, using the smallest reactant models, namely succinic anhydride **5** and *N*-methyl methyleneimine **6**. For the computations of the simplest examples of dicarboxylic anhydride iminolysis we apply DFT,[11] using the B3LYP hybrid functional with the 6-31G*, 6-311G**, and cc-pVTZ basis sets, and MO theory[12] at the MP2/6-31G* level. In the case with imine attack on the nonenolized succinic anhydride, we find a transition structure, TS **7**, also envisaged earlier,[1] which corresponds to the *keto* form of anhydrides **1** or **5** (see Scheme 2).

SCHEME 2. Computed Reaction Species for CH_3-N=CH_2 Addition to Keto-succinic Anhydride[a]

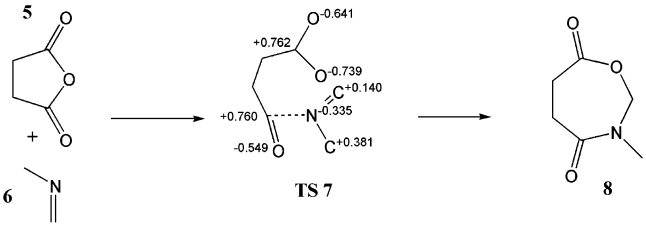

6 **TS 7** **8**

[a] NBO charges on **TS 7**, B3LYP/cc-pVTZ, indicate no zwitterionic charge distribution.

However, an IRC[13] calculation shows that **7** connects the initial anhydride **5** and imine **6** to a seven-membered 3-oxazepidine-4,7-dione **8**[1] and not to the target pyrrolidinone or quinolinone (Schemes 2 and 1, respectively). The distribution of NBO[14] charges on located TS **7** does not resemble the expected one for zwitterionic species **3** or **4**, postulated as intermediates by Cushman and Madai.[7] The smooth unimodal IRC energy profile indicates that the iminolysis of keto-succinic anhydride by Schiff base (Scheme 2) would be a concerted approximately thermoneutral reaction with no intermediates (see also Table 1).

Another model attack is then pursued on the enol form of succinic anhydride **9**. Imine **6** attack on the nonenolized carbonyl atom of **9** does indeed produce a different TS, **10**, resembling in topology the structure postulated for intermediates of the studied reaction (Scheme 3).[7] However, like TS **7**, TS **10** has no zwitterionic charge distribution. IRC calculations starting from **10** result

TABLE 1. B3LYP/cc-pVTZ Results on H_2C=NCH_3 Addition to Succinic Anhydride[a]

species	B3LYP/ cc-pVTZ	$E + \Delta G$, au	ΔG	N_{imag} (ν)	ZPE
H_2C=NCH_3 **6**	−133.99503	−133.95192		0	42.57
anhydride **5**	−380.66893	−380.62077	0	0	49.42
anhydride enol **9**	−380.63390	−380.58566	22.0	0	48.93
TS-keto **7**	−514.61333	−514.49862	46.5	1 (−173.7)	93.98
TS-enol **10**	−514.59209	−514.47854	59.1 (37.0)	1 (−212.0)	92.94
adduct **8**	−514.68214	−514.56372	+5.6	0	96.49
adduct **11**	−514.70049	−514.58378	−7.0 (−29.0)	0	96.08

[a] N_{imag} is the number of imaginary vibrational frequencies. δG and ZPE in kcal·mol^{-1}. Imaginary frequencies are given in parentheses, cm^{-1}. ΔG in parentheses are free energies relative to the anhydride enol **9.**

SCHEME 3. Computed Reaction Species for CH_3N=CH_2 Addition to Succinic Anhydride Enol[a]

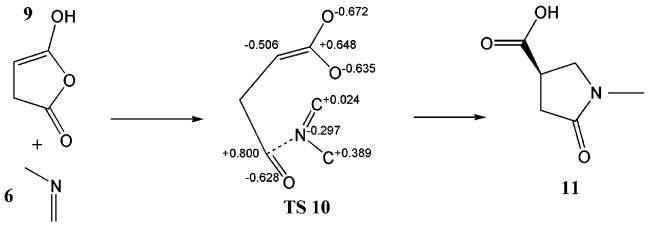

6 **TS 10** **11**

[a] NBO charges on **TS 10**, B3LYP/cc-pVTZ, indicate no zwitterionic charge distribution.

once again in a smooth unimodal energy profile starting from the reactants **6** + **9** and ending with the five-membered adduct **11**, structurally corresponding to the experimentally obtained products of succinic anhydride iminolysis, substituted pyrrolidinones[1] (Scheme 3). Thus, the latter IRC energy profile shows no intermediate as well and represents another concerted reaction.

The Perkin-like mechanistic alternative is a multistep reaction, proceeding initially via the anhydride enol **9** to form the aldol-like intermediate with a relatively low activation energy, which is even more stable than **8**. The second ring closure step however requires a significantly higher activation energy (Table S1, Supporting Information). Thus, the resulting stepwise reaction energy profile does not seem to fit the experimentally observed exothermic processes proceeding in a matter of seconds.[7]

The two mechanistic alternatives—concerted imine addition plus intramolecular charge transfer cyclization vs the Perkin-like stepwise addition—occur via the enol form **9** of succinic anhydride. The direct enolization step of the process, however, should involve suprafacial migration of α-hydrogen and is thus symmetry forbidden. According to our calculations, the respective transition structure is ca. 80 kcal/mol higher than **5**, B3LYP/cc-pVTZ. The thermodynamic equilibrium ratio of enol **9** vs anhydride **5** should thus be ca. 10−16, and any higher concentration of enol **9** can be inferred completely as the result of bimolecular processes, e.g., in the present case "unproductive" collisions of anhydride **5** and imines **6**, **12**, or **13**, which is evidently sufficient to start the reaction. The products, carboxylic acids, then sustain the enolization process even in nonionizing reaction media.[1,7,10]

(10) Kozekov, I. D.; Koleva, R. I.; Palamareva, M. D. *J. Heterocycl. Chem*. **2002**, *39*, 229. Koleva, R. I. Ph.D. Thesis, Faculty of Chemistry, University of Sofia, 2002.

(11) Koch, W.; Holthausen, M. C. *A Chemist's Guide to Density Functional Theory*; Wiley-VCH: Weinheim, New York, 2000.

(12) Hehre, W. J.; Radom, P.; Schleyer, P. v. R.; Pople, J. A. *Ab Initio MO Theory*; Wiley: New York, 1986.

(13) Gonsalez, C.; Schlegel, H. B. *J. Chem. Phys.* **1989**, *90*, 2154; *J. Chem. Phys.* **1990**, *94*, 5523.

(14) Reed, A. E.; Curtiss, L. A.; Weinhold, F. *Chem. Rev.* **1988**, *88*, 899.

TABLE 2. MP2/6-31G* Results on $H_2C{=}NCH_3$ Addition to Succinic Anhydride[a]

species	MP2/6-31G*	$E + \Delta G$	ΔG	N_{imag} (ν)	ZPE
$H_2C{=}NCH_3$ **6**	−133.47887	−133.43368	–	0	43.88
anhydride **5**	−379.44838	−379.39715	0	0	50.43
anhydride enol **9**	−379.40248	−379.35347	0 (28.8)	0	49.55
TS-keto **7**	−512.88168	−512.76234	43.0	1 (−168.6)	96.66
TS-enol **10**	−512.85378	−512.73603	32.1	1 (−197.1)	95.28
adduct **8**	−512.95703	−512.83491	−2.6	0	98.99
adduct **11**	−512.98404	−512.86339	−47.8	0	98.55

[a] N_{imag} is the number of imaginary vibrational frequencies. Absolute energies in au. ΔG and ZPE in kcal·mol^{-1}. Imaginary frequencies are in parentheses, cm^{-1}.

The synthetically observed product (Scheme 3) is thus the result of a moderately exothermic reaction having a completely new mechanism, namely concerted addition of imine **2** to the remaining keto (carboxylic) group of enolized anhydride **9**, accompanied by simultaneous elimination of carboxylate. A problem remaining with this mechanism is the energetic one. Calculations show that the keto-reaction path lies in general lower than the enolic path, see Table 1 and Figure 1, even though the activation energy of the enolic path is lower. Another problem concerns the driving force for the smooth contiguous energy profile of the reaction after TS **10**. Note that with the used basis sets, the calculated free energy differences (Table 1; Tables S1 and S2, Supporting Information) apparently become smaller from 6-31G* to 6-311G**, and the largest cc-pVTZ. Calculated reaction thermodynamics are approximately the same at B3LYP/6-311G** and B3LYP/cc-pVTZ, with no qualitative discrepancy between 6-31G* and cc-pVTZ.

To independently check the mechanism suggested by DFT calculations, we repeat the same stationary point search on the reaction potential energy surfaces by MP2/6-31G* calculations. For the iminolysis reaction of **5** and **6**, we obtain a TS with the topology of **7**. The MP2/6-31G* iminolysis reaction with the enol **9** leads to another TS with the topology of **10** and then smoothly to the pyrrolidinone **11**, as described above for the B3LYP/cc-pVTZ calculation. Energetically, both B3LYP and MP2 energy profiles for the iminolysis of keto-anhydride **5** are invariably lower than those for the iminolysis of the enol **9**. Another similarity is that activation energies for **9** to TS **10** are significantly lower than for **5** to TS **7**. Enolization free energies are lower than the keto-iminolysis activation energy as well (Table 2, Figure 1). The only quantitative difference found between the two types of theory is that MP2 activation energies are uniformly lower than B3LYP values. Thus, we find no qualitative difference between the two types of theory, MO and DFT. Therefore, one can rely on DFT calculations in further studies of dicarboxylic anhydride iminolysis, as shown also by our "real size model" B3LYP and MP2 calculations hereafter.

Present calculations using the two types of theory show reliably that the observed reaction of Schiff bases with succinic anhydride giving pyrrolidinones is a fine example of competing reactions of *keto*- and *enol*-anhydride isomers. The equilibrium amount of the latter isomer can be expected very low (Tables 1 and 2), while the calculated thermochemical effect of its iminolysis is significantly larger. Another reason the enol reaction to prevail under experimental conditions is autocatalysis, since the iminolysis product is a carboxylic acid promoting further enolization.[7]

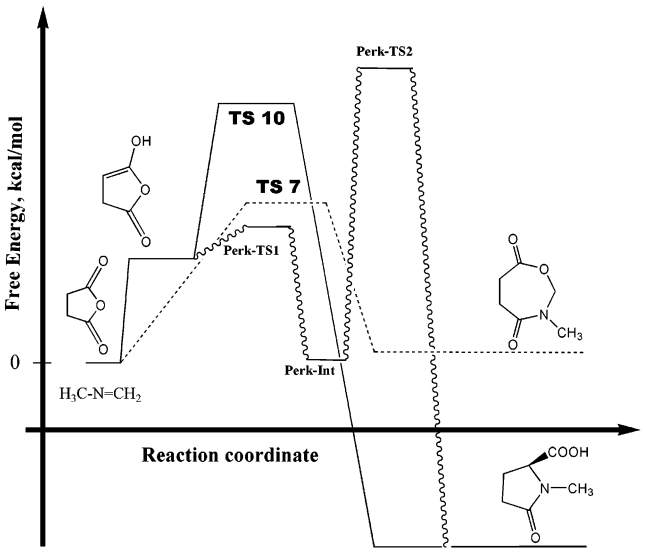

FIGURE 1. Qualitative free energy profiles for Schiff base ($CH_3N{=}CH_2$) iminolysis of succinic anhydride, B3LYP/cc-pVTZ and MP2/6-31G* (not to scale): solid line: *enol*-iminolysis; dotted Line, *keto*-iminolysis. The squiggly line represents the alternative Perkin-like addition; see also Figure S7 (Supporting Information).

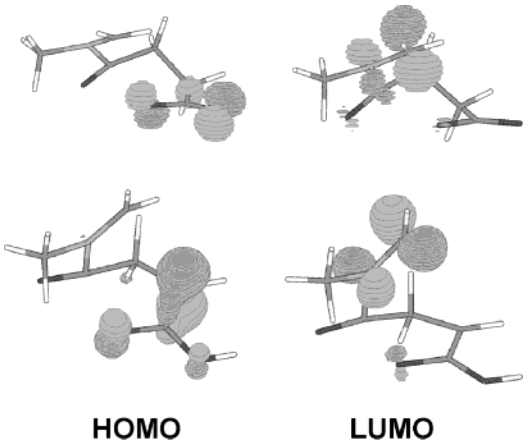

FIGURE 2. Frontier orbitals of **TS 7**, top, and **TS 10**, bottom, B3LYP/6-31G*.

Are there electronic reasons for the concertedness of dicarboxylic anhydride iminolysis? To address this problem, we examine first the π-orbitals of TS **7** and TS **10**. Both MO MP2/6-31G* and DFT B3LYP/cc-pVTZ calculations show that the HOMOs of the two transition structures are localized on the carboxylate of **7**, respectively, carboxylate enol group of **10**. The LUMOs are in turn localized on the quaternized azomethine group, Figure 2. Thus, intramolecular through-space charge transfer becomes highly probable, as indicated also by the relatively small difference between HOMO and LUMO energies, 2.69 eV for **TS 7**, and 2.76 eV for **TS 10**, B3LYP/cc-pVTZ.

14 **15**

FIGURE 3. Transition structures arising from succinic anhydride iminolysis by (*E*)-, **14**, and (*Z*)-$C_6H_5CH{=}NCH_3$, **15**, B3LYP/6-311G**.

TABLE 3. B3LYP/6-311G Results on $C_6H_5CH{=}NCH_3$ Addition to Succinic Anhydride[a]**

species	B3LYP/ 6-311G**	$E + \Delta G$	ΔG	N_{imag} (ν)	ZPE
anhydride **5**	−380.62831	−380.57884		0	49.32
anhydride enol **9**	−380.59222	−380.54404	21.8	0	48.92
E-PhCH=NCH_3 **12**	−365.10040	−364.98378		0	93.75
Z-PhCH=NCH_3 **13**	−365.08849	−364.97178		0	93.92
TS **14**	−745.64246	−745.45594	66.9 (45.1)	1 (−354.4)	143.17
TS **15**	−745.65216	−745.46412	54.3 (32.4)	1 (−213.8)	144.13
adduct **16**	−745.75692	−745.56541	−1.8 (−23.6)	0	146.75
adduct **17**	−745.75092	−745.55943	−5.5 (−27.4)	0	146.68

[a] N_{imag} is the number of imaginary vibrational frequencies. Absolute energies in au. ΔG and ZPE in kcal·mol^{-1}. Imaginary frequencies are in parentheses, cm^{-1}. ΔG in parentheses are relative to the enol **9.**

It is indeed of more interest to study a "real size model" to show the ability of contemporary theory to not only reliably explain the reaction mechanism, but to predict reaction stereochemistry as well. For this purpose, we use B3LYP/6-311G** and MP2/6-31G* calculations of succinic anhydride enol iminolysis by benzylidene methylamine[1] $C_6H_5CH{=}NCH_3$ **12** (the *E*-isomer) and **13** (the *Z*-isomer). As expected, the transition structure search results in two structures, TS **14** and TS **15**, similar to TS **7** and **10** above (Figure 3). Using the energetically preferred mechanism (Scheme 3), one can deduct two factors assisting stereoselectivity of this reaction: the *E*/*Z* isomerism of Schiff bases and the reaction concertedness manifested by the still existing anhydride ring during the still incomplete imine addition, which ensures attack of the prochiral imine carbon on one face of the prochiral enol carbon only (Figure 3). The two TS's **14** and **15** have two prochiral carbon atoms with Re,Si (**ul**) and Re,Re (**lk**) relative orientations,[15] respectively, the incipient bonding of which is to give correspondingly the *trans*- and *cis*-pyrrolidinone adducts **16** and **17**, with clear thermodynamic preference for the former product. Experimentally, the major product of the reaction is indeed **16**.[1] However, calculated B3LYP/6-311G** theoretical activation free energies, Table 3, as well as the MP2/6-31G* values are lower for TS **15**. Thus, the theoretically preferred diastereoisomeric reaction pathway would produce the cis product **17** in apparent contradiction to experimental findings.

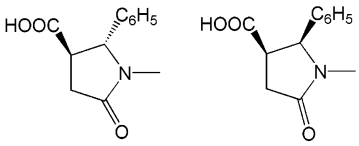

16 **17**

Careful inspection of theoretical transition structures (Figure 3) reveals that TS **14** for the *E*(*trans)*-diastereoisomer is somewhat more advanced toward ring closure than the respective *Z(cis)*-structure of TS **15**: the incipient C···C bond distance in **14** is 2.791 Å (N···C = 1.826 Å, C···O = 1.846 Å), while for **15** this distance is 2.884 Å (N···C = 1.646 Å, C···O = 1.792 Å, MP2/6-31G*; see the broken lines in Figure 3). At the B3LYP/6-311G** level, the corresponding geometry parameters are C···C, 2.361 Å, N···C, 1.911 Å, C···O, 1.751 Å for **14** and C···C, 3.117 Å, N···C, 1.690 Å, C···O, 1.807 Å for **15**. Thus, notwithstanding numerical differences, both types of theory—MP2 and DFT/B3LYP—predict somewhat more advanced addition part of the reaction for the *Z*-isomer **15**, but more advanced heterocyclic ring closure toward the trans adduct **16**. The reported product distribution stereochemistry[1,7] refers to the thermodynamically controlled process, while the kinetically controlled imine addition produces the cis adduct **17**,[1,10] which is capable of later epimerization to **16**[7,10] to give the thermodynamically controlled product. Similar results, showing the *Z*-transition structure as more stable, are obtained by diffuse basis set B3LYP/6-31+G* gas phase and single-point SCRF[16] B3LYP/6-31G* solvent calculations for the same model in benzene; see the Supporting Information.

The important finding with the two diastereoisomeric TS's **14** and **15**, having little spatial similarity, is that their respective electronic structure features, in particular the localization of donor HOMO and acceptor LUMO enabling the ring closure, remain similar enough. Thus, the calculational prediction for a more rapid formation of the cis adduct **17** under kinetic control is at least in qualitative agreement with experiments[1,10] and encourages further theoretical studies in the stereochemistry of imine cycloadditions to higher, e.g., homophthalic **1**, anhydrides.

Our computational study shows, that the rate-determining step of dicarboxylic anhydride iminolysis by Schiff bases is a concerted reaction, starting as a nucleophilic addition of imine to the carbonyl carbon of anhydride enol with concomitant elimination of carboxylate, while completing as an intramolecular charge transfer with ring expansion and closure. The preliminary anhydride enolization step is an equilibrium, supplying the reactive "intermediate" enol **9**.

Supporting Information Available: Tables with full B3LYP and MP2 results; Figures with IRC energy profiles and geometries. This material is available free of charge via the Internet at http://pubs.acs.org.

JO034240J

(15) Prelog, V.; Helmchen, G. *Helv. Chim. Acta* **1972**, *55*, 2581. Prelog, V.; Helmchen, G. *Angew. Chem., Int. Ed. Engl.* **1982**, *21*, 567. Seebach, D.; Prelog, V. *Angew. Chem.* **1982**, *94*, 696.

(16) Kirkwood, J. G. *J. Chem. Phys.* **1934**, *2*, 351. Onsager, L. *J. Am. Chem. Soc.* **1936**, *58*, 1486. Tomasi, J.; Persico, M. *Chem. Rev.* **1994**, *94*, 2027.